

# Identification of photodegradants of droloxifene by combined HPLC–MS, NMR spectroscopy and computational chemistry

Anthony M. Campeta,\* Franco Lombardo, Thomas R. Sharp, George J. Horan and Diane M. Rescek

Pfizer Inc., Central Research Division, Groton, Connecticut 06340, USA

Received 13 July 1999; accepted 13 July 1999

**ABSTRACT:** A combination of high-performance liquid chromatography (HPLC)–mass spectrometry and  $^1\text{H}$  and  $^{13}\text{C}$  NMR spectroscopy was utilized to characterize the photodecay products of droloxifene, a potent new estrogen receptor agonist. Structurally similar to tamoxifen, droloxifene demonstrates a complex and unique decay scheme, including the formation of two naphthalene derivatives which were unexpected decay products and previously unreported for this class of compound. Elucidation of the decay products was assisted by the use of computational chemistry, namely by correlating simulated UV spectra and aqueous solvation free energies with actual UV spectra and HPLC retention data. In addition to describing the photodecay scheme of droloxifene, the present work demonstrates the utility of computational chemistry in providing support for the identification of unknown compounds. Copyright © 1999 John Wiley & Sons, Ltd.

**KEYWORDS:** NMR;  $^1\text{H}$  NMR;  $^{13}\text{C}$  NMR; droloxifene; photodegradants; liquid chromatography–mass spectrometry

## INTRODUCTION

Droloxifene (Fig. 1,  $\text{R} = \text{OH}$ ) is a potent new estrogen receptor agonist which is targeted for the treatment of osteoporosis. It is a derivative of triphenylethylene, and similar in structure to the commercially available drug tamoxifen ( $\text{R} = \text{H}$ ). Stability studies of droloxifene in solution have revealed the compound to be extremely unstable in the presence of light. Furthermore, the decay scheme in light is complex, with the appearance of 4–6 major decay products over time, depending upon pH. Photochemical conversion of tamoxifen and droloxifene to phenanthrene derivatives to increase sensitivity for fluorescence-based serum assays has been reported.<sup>1,2</sup> In the case of tamoxifen, structural identity of these

phenanthrenes has been clearly made.<sup>3,4</sup> However, the complete photodegradation profile of droloxifene or any other triphenylethylene compound has not been formally reported. The purpose of this study was to elucidate the photodegradation pathways of droloxifene and provide identification of the degradation products therein.

## EXPERIMENTAL

### Materials

Droloxifene, as the citrate salt, and its corresponding geometric *Z*-isomer were obtained from Klinge Pharma GmbH (Munich, Germany). Based on the attached group priorities on the aromatic rings of the molecule, droloxifene carries the *E* stereochemical designation. Acetonitrile, methanol (J.T. Baker, Phillipsburgh, NJ, USA) and trifluoroacetic acid (Sigma Chemical, St Louis, MO, USA) were of high-performance liquid chromatography (HPLC) grade. Hydrochloric and phosphoric acid (J.T. Baker) were of reagent grade. High-purity water was obtained from a Milli-Q water system (Millipore, Bedford, MA, USA).

### Sample preparation and storage

For assessment of stability in light, solutions of droloxifene were prepared in 0.06 M hydrochloric acid (pH 1.5) and 0.02 M sodium phosphate–sodium acetate

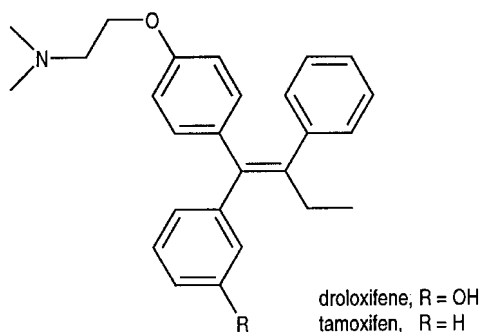


**Figure 1.** Structure of droloxifene and tamoxifen

\*Correspondence to: A. M. Campeta, Pfizer Inc., Central Research Division, Groton, Connecticut 06340, USA.

buffer (pH 3.0, 5.0 and 7.0). Acetonitrile was added to these solutions (20%, v/v) to allow a droloxifene concentration of  $75 \mu\text{g ml}^{-1}$  throughout the pH range. These solutions were stored in clear glass vials (1.5 ml) and sealed with Teflon-lined plastic screw caps. Photodegradation was carried out by storing the vials in an 840 foot-candle fluorescent light cabinet constructed in-house, maintained at  $30^\circ\text{C}$ . Vials were periodically removed and assayed by HPLC.

To generate milligram quantities of two late-eluting droloxifene degradants for NMR analysis, a  $10 \text{ mg ml}^{-1}$  solution of droloxifene in buffer at pH 3.0 (with 20% acetonitrile) was subjected to storage in light as above for 8 months. Most of the two desired degradants that were formed precipitated from this solution. The resulting suspension was filtered. The retained solid was washed with several portions of water, then dissolved in a minimum amount of acetonitrile–water (80:20). This solution was injected into the semi-preparative HPLC system described below. Fractions of each pure compound were collected and pooled after each injection.

For NMR analysis, each of the above compounds was extracted from solution with either diethyl ether or carbon tetrachloride. The solvent solutions were then dried with magnesium sulfate, filtered and evaporated to dryness. Each degradant solid was dissolved in 0.6 ml of deuterated acetonitrile for NMR analysis. The extraction procedure was repeated with blank solvent and run as a control.

## HPLC analysis

Degradation of droloxifene was monitored using an HPLC method which was developed to permit the separation of droloxifene from all of its light-induced decay products. This chromatographic system utilized a Thermo Separation Products ConstaMetric 3200 isocratic pump and an Applied Biosystems Model 785 programmable-wavelength UV detector set at 230 nm. Samples were injected using a Bio-Rad AS-100 autoinjector equipped with a  $20 \mu\text{l}$  injection loop. Data were collected and tabulated utilizing a TurboChrom (P.E. Nelson) data acquisition software platform (version 4). The column was a Beckman Ultrasphere  $\text{C}_{18}$  with dimensions of  $250 \times 4.6 \text{ mm i.d.}$ , maintained at  $30^\circ\text{C}$  with a Bioanalytical Systems LC-22C column heater. The isocratic mobile phase consisted of water–methanol–acetonitrile–trifluoroacetic acid (47:30:23:0.1, v/v adjusted to pH 3 with ammonium hydroxide solution) and was delivered at  $1.5 \text{ ml min}^{-1}$ . The mobile phase was filtered and degassed prior to use. UV spectra were obtained for decay products with a similarly instrumented HPLC system as described above with an identical mobile phase except that it was equipped with a Bio-Rad Bio-Dimension Scanning UV–visible diode-array detector.

Two late-eluting droloxifene degradants were col-

lected from multiple HPLC injections for NMR analysis, using the same HPLC equipment as above and a semi-preparative column from the same manufacturer having dimensions of  $250 \times 10 \text{ mm i.d.}$  A mobile phase ratio of 45:25:20:0.1 (v/v) (solvents as above) was utilized and delivered at  $5 \text{ ml min}^{-1}$ . Injected sample volumes were typically  $300 \mu\text{l}$ . Targeted degradants were recovered as described above.

## HPLC–mass spectrometric (MS) analysis

Atmospheric pressure chemical ionization (APCI) experiments were performed on a Fisons Instruments Quattro triple-quadrupole mass spectrometer, using the HPLC separation system described above on a Hewlett-Packard Model 1050 quaternary HPLC system. Static and dynamic mass spectrometer calibrations were performed in the electron ionization mode against perfluorotributylamine, and checked in the APCI mode with a solution of polyethylene glycol. APCI interface and mass spectrometer tuning parameters were optimized for droloxifene by repeated flow injections. For MS–MS collision-induced decomposition (CID) studies, argon was used in the collision cell.

## $^1\text{H}$ and $^{13}\text{C}$ NMR analysis

One- and two-dimensional NMR experiments were performed to identify the structures of two of the droloxifene degradants which could not be intuitively discerned from mass spectral and UV spectral analysis. A Bruker DMX500 instrument with  $z$ -gradients using a 5 mm broadband inverse probe was used to acquire proton, carbon, DEPT (distortionless enhancement by polarization transfer), gradient COSY (correlation spectroscopy), gradient HMQC (heteronuclear multiple quantum correlation spectroscopy), long-range gradient HMQC, and NOE (nuclear Overhauser effect) data<sup>5</sup> at  $25^\circ\text{C}$ . The long-range gradient HMQC experiment was optimized for 6 Hz, which is the average  $J$  coupling for three bonds [ $J(\text{C},\text{C},\text{C},\text{H})$ ] in aromatic systems and two bonds [ $J(\text{C},\text{C},\text{H})$ ] in aliphatic systems.

## Computational methods

Computed aqueous solvation free energies ( $\Delta G^\circ_{\text{w}}$ ) were calculated for correlation with HPLC retention data using the Cramer–Truhlar SM2 solvation model, implemented in the SPARTAN software package.<sup>6</sup> For the phenanthrenes I, II and III the solvation energy was computed on the neutral molecule, although the side-chain nitrogen atom would be protonated under the elution conditions. This is a reasonable simplification, as the side-chain is likely to exert the same effect on the capacity factor for

each compound, and not to influence the interaction of the aromatic portion of the molecule with the stationary phase in a significantly different way for any of the isomers.

Using the Sybyl ForceField computation, as implemented in the Sybyl software package<sup>7</sup> (version 6.3), a systematic conformational search was performed on diastereomers **6** and **7**. The dihedral angle of the bond connecting the carbonyl to the olefinic carbons was incremented by 180° (*s-cis* or *s-trans*), while the torsional angles of the remaining bonds (the bond connecting the naphthalene to the phenolic ring and the bond connecting the naphthalene to the olefinic carbon) were searched using 15° increments. An energy window of 3 kcal mol<sup>-1</sup> (1 kcal = 4.184 kJ) was used to filter out high energy conformers. The resulting structures were then partitioned into families using the dihedral angle values as criteria, and the lowest energy conformer from each family was selected out and minimized. This procedure resulted in eight representative compounds for each diastereomer. These representative compounds were subsequently imported into CaChe,<sup>8</sup> and were used to compute simulated UV spectra (gas phase) using the ZINDO molecular orbital package.

## RESULTS AND DISCUSSION

### Photostability and kinetics

Figure 2 shows a typical HPLC trace for droloxifene degraded in light in a pH 3 solution. This solution represents about 85% decomposition of droloxifene,

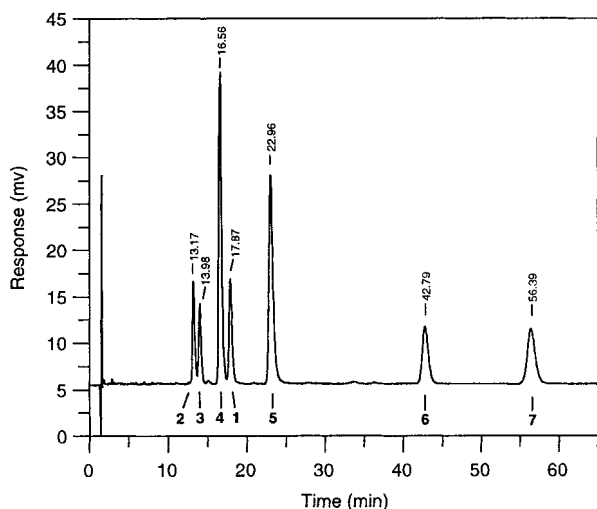


**Figure 2.** HPLC trace for the pH 3 droloxifene solution exposed to light for 1 week. 1 = Droloxifene; 2 = phenanthrene I; 3 = droloxifene Z-isomer; 4 = phenanthrene II; 5 = phenanthrene III; 6 = Z-naphthalene derivative; 7 = E-naphthalene derivative. See text for explanation of structural and peak assignments)

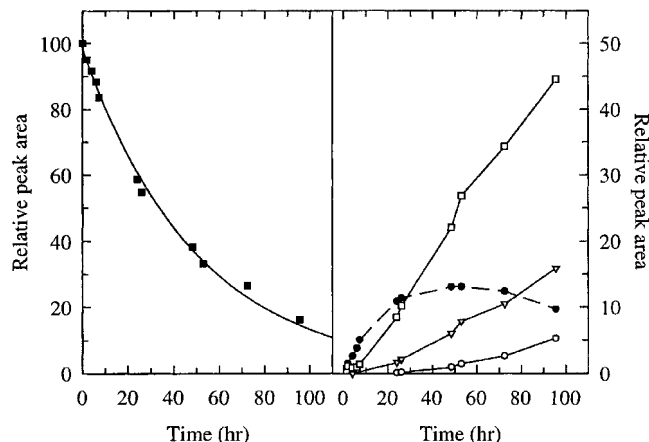


**Figure 3.** Apparent first-order decay of droloxifene (■) in light-exposed (840 foot-candle) pH 1.5 solution at 30°C and formation of degradants, **2** (○), **3** (●), **4** (□) and **5** (▽). Compounds **6** and **7** precipitated from solution during the study and are not shown

which elutes at 17.8 min in the assay. As shown, there are six major decay products which appear over time. The rate of appearance of the two most highly retained degradants, eluting at approximately 43 and 56 min, diminished as the pH of the solution increased until they were no longer produced in pH 7 solution. The rate of decay was generally very fast, following an apparent overall first-order process, as shown in Fig. 3. The typical half-life for droloxifene decay was 36 h in pH 1.5 solution and 60 h in pH 3, 5 and 7 solutions.

### Mass spectrometric behavior of droloxifene

The APCI mass spectrum of droloxifene showed a prominent  $[M + H]^+$  ion at  $m/z$  388 with no other significant features. MS-MS CID of droloxifene did not produce very informative product ion spectra. The only reliably abundant fragment appeared at  $m/z$  72, which corresponds to the *N,N*-dimethylaminoethyl side-chain. This behavior is identical with that reported for tamoxifen.<sup>9</sup> A number of different collision energy and collision gas density conditions were explored in a search for more useful CID conditions, without success.

### Identification of decay products 2-5

LC-MS was used as the primary method for initial structural identification of the degradants. Much of the photochemistry expected for tamoxifen and droloxifene parallels that for stilbene derivatives, which have been extensively studied.<sup>10</sup> Upon exposure to light, it has been shown that tamoxifen isomerizes to its corresponding geometric isomer, with each isomer capable of undergoing a cyclization reaction with a loss of two hydrogen

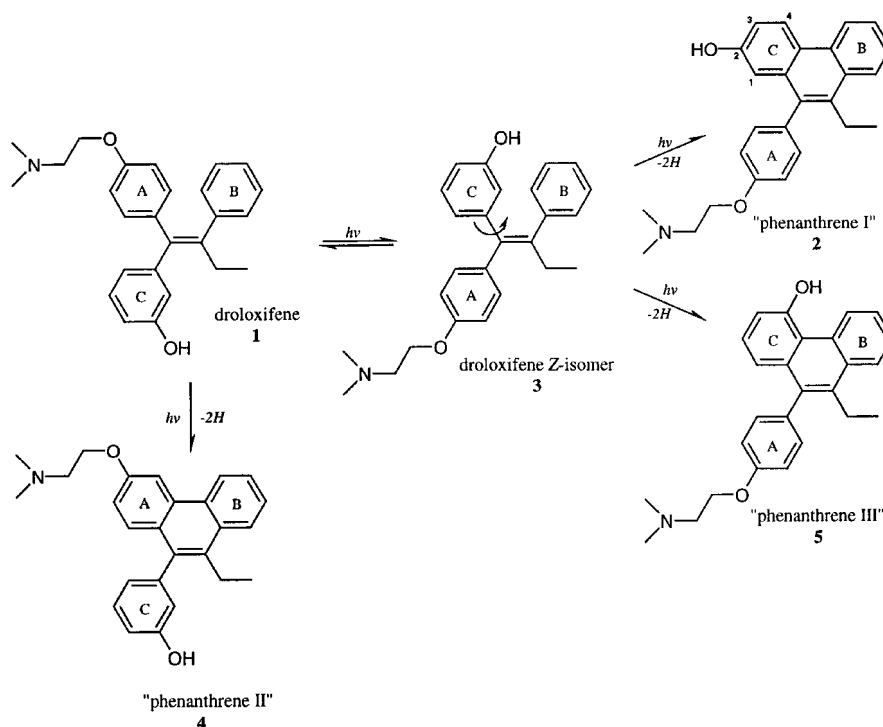


**Figure 4.** Proposed formation of phenanthrenes from droloxifene photodegradation

atoms to form a corresponding phenanthrene analog.<sup>4</sup> A similar behavior was also expected for droloxifene.

Referring to Fig. 2, analysis of compound **3** demonstrated a mass spectrum and a UV spectrum identical with those of droloxifene. Ultimately confirmed by HPLC co-elution with an authentic sample, **3** was identified as the *Z* geometric isomer of droloxifene (see Fig. 4).

APCI mass spectra of the chromatographic peaks for **2**, **4** and **5** showed a prominent  $m/z$  386 species, two mass units below that of droloxifene, and the expected  $[M + H]^+$  for a phenanthrene analog. The mass spectra of the three chromatographically separated compounds were indistinguishable from each other. Unlike tamoxifen, where only two phenanthrene compounds may form on exposure to light, structural examination of droloxifene suggested that the formation of three phenanthrene compounds was possible. Droloxifene itself should produce phenanthrene II, shown in Fig. 4, where rings A and B have been fused into the phenanthrene nucleus. The formation of the additional two phenanthrenes first requires isomerization of droloxifene to its *Z*-isomer. These latter two phenanthrenes then originate from the fact that, prior to ring fusion, ring C is free to rotate about its bond to the central olefin. The asymmetry created due to the *meta* positioning of the hydroxyl group on this ring leads to two possible positional isomers, shown as phenanthrenes I and III in Fig. 4. Formation of positional phenanthrene isomers in this manner has been demonstrated for other asymmetrically substituted stilbene derivatives.<sup>11</sup> As mentioned, LC-MS alone could not distinguish which of the chromatographic peaks corre-

sponded to each of the three phenanthrene analogs. Assignments were achieved through the use of the computational chemistry methods described below.

### Assignment of phenanthrene isomers

As shown in Fig. 3, the extent of formation of the three phenanthrene degradants typically followed the order **4** > **5** > **2**. Since it was produced in greatest abundance, **4** was proposed intuitively to originate from the starting droloxifene isomer (*E*-isomer), and the other two phenanthrenes from the droloxifene *Z*-isomer. This notion was supported kinetically by the fact that photodegradation of droloxifene *Z*-isomer as the starting material resulted in the formation of significantly higher levels of **5** and **2** relative to **4**. By analogy with some of the physical and chemical properties of tamoxifen and related phenanthrene compounds present in the literature, some evidence was available to support these assignments. Coupled with the use of computational approaches, particularly the use of computed aqueous solvation free energies ( $\Delta G^\circ_w$ ) as a measure of each compound's relative polarity, consistent evidence was obtained ultimately to provide highly confident structural assignments.

The UV spectra of **2**, **4** and **5** are shown in Fig. 5. Each compound displayed a prominent absorption band between 250 and 260 nm, with the overall UV profile consistent with hydroxylated phenanthrenes<sup>12</sup> and those phenanthrenes derived from tamoxifen.<sup>4</sup> As a potentially

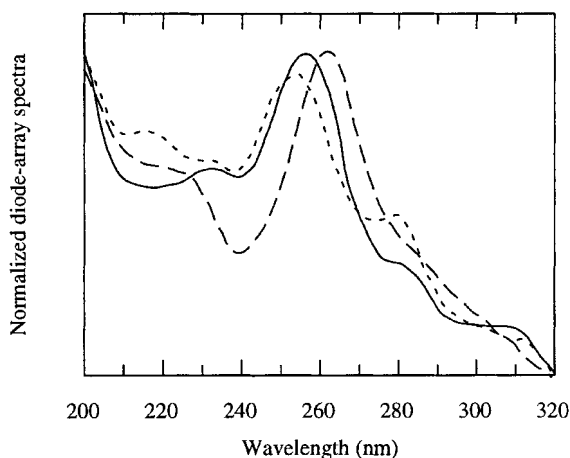


**Figure 5.** UV Spectra for compounds **2** (---), **4** (—) and **5** (— · —)

useful first approach, the UV spectra of the three proposed phenanthrene structures were calculated through computer modeling, then compared with the actual spectra of the proposed phenanthrene compounds **2**, **4** and **5**. The modeling of phenanthrene structures I, II and III accurately produced spectra with  $\lambda_{\text{max}}$  values within 4 nm of experimental values on average, which supported their structural assignment. However, owing to the structural similarities of the three phenanthrene isomers and the resulting closeness of their experimental  $\lambda_{\text{max}}$  values (Fig. 5), differentiation using the computed spectra was difficult. In addition, some of the more subtle absorption bands in the actual spectra were not captured by the simulated spectra, which made it difficult to 'fingerprint' the three compounds. Hence the spectral simulations, although fairly accurate in modeling the experimental spectra, could not be used to assign definitively the structures of each isomer.

The UV spectra of the phenanthrenes identified from the photodecomposition of tamoxifen and its geometric isomer<sup>4</sup> had distinguishing characteristics which were very similar to the spectra of **4** and **5**, respectively. Owing to structural similarities between droloxifene and tamoxifen, their respective phenanthrene degradants would be expected to have very similar UV spectra. In addition, the phenanthrene derived from tamoxifen is more polar than that derived from its geometric isomer based on reversed-phase HPLC retention,<sup>4</sup> which corresponds to **4** being more polar than **5** (Fig. 2). Taken together and considering the kinetic data, these correlations support **4** as being the phenanthrene originating directly from droloxifene, i.e. phenanthrene II in Fig. 4, and **5** and **2** as originating from the droloxifene Z-isomer.

Owing to the relative uniqueness of droloxifene in producing three phenanthrene degradants, no literature evidence was available to differentiate directly the phenanthrenes derived from the droloxifene Z-isomer, namely **2** and **5**. This was accomplished through an

examination of the relative polarities of the two proposed structures. The molecules were expected to differ only in the position of a ring hydroxyl group at either the 2- or 4-position (Fig. 4). The hydroxyl at the 2-position should be more solvent accessible. Hence this compound should be more polar and less retained on reversed-phase HPLC. Indeed, this has been demonstrated for a series of hydroxyphenanthrenes, where 2-hydroxyphenanthrene was shown to elute much earlier than 4-hydroxyphenanthrene on C<sub>18</sub> reversed-phase columns.<sup>12</sup> Compound **2** is significantly more polar than **5**, as shown in Fig. 2, suggesting that the former is the 2-hydroxyphenanthrene derivative and the latter the 4-hydroxy derivative (phenanthrenes I and III, respectively, Fig. 4).

Computer modeling was then used to lend support to the above arguments, in an attempt to differentiate further these latter two phenanthrene derivatives. The computed aqueous solvation free energy of each proposed structure, a measure of their relative polarities, was calculated and compared with the HPLC retention order of each phenanthrene peak. As can be surmised from their relatively large difference in HPLC retention (Fig. 2), phenanthrenes I and III must differ significantly in polarity. Calculated solvation free energies ( $\Delta G^\circ_{\text{w}}$ ) were therefore expected to be largely different and predictive of their relative HPLC retention times. The calculated solvation free energy was indeed significantly different for phenanthrenes I and III, with values of  $-10.20$  and  $-8.85$  kcal mol<sup>-1</sup>, respectively. This suggests that the better solvated structure (more negative value) is phenanthrene I, and this compound would be expected to be less retained on a reversed-phase HPLC column. On the other hand, phenanthrene II elutes more closely to phenanthrene I and it was thought to be more difficult to 'separate' by means of its solvation free energy from the other phenanthrenes I and III. Phenanthrene II showed no difference from I in solvation free energy, with a computed value of  $-10.20$  kcal mol<sup>-1</sup>. However, on the basis of the kinetic observations and the mechanistic arguments proposed, the distinction between I and III can be made and allows the assignment of all three phenanthrenes to the chromatographic peaks. Incidentally, the commonly used CLogP<sup>13</sup> and SRC LogKow<sup>14</sup> prediction packages could not distinguish between any of the phenanthrenes, as might be expected from the fragmental nature of most of those calculation methods. Thus, taken with the kinetic data and all other supportive arguments that have been discussed, the decay compounds **2**, **4** and **5** can be assigned as the three phenanthrene derivatives I, II and III, respectively, shown in Fig. 4.

### Identification of acidic decay products 6 and 7

In acidic pH media, namely pH 1.5, 3 and 5 solutions, two additional highly retained decay products were formed

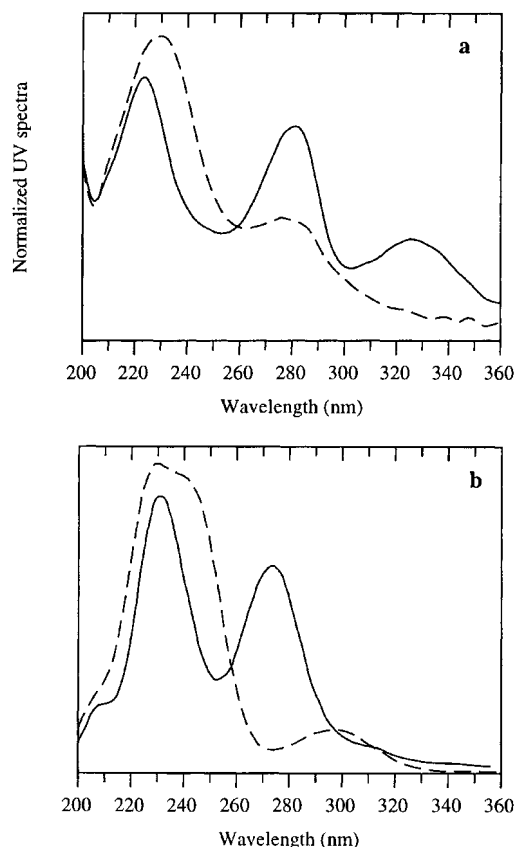


**Figure 6.** (a) Experimental and (b) simulated UV spectra of compounds **6** (---) and **7** (—). The simulated spectra were performed on their proposed structures shown in Fig. 7

over time. These products were produced in nearly similar quantities in the pH 1.5 and 3 solutions. Approximately one-tenth lower levels were produced in the pH 5 solution. The products were not formed at all at pH 7. The two products, when formed in each respective solution, were produced in almost identical abundance over time. The UV spectra of these products were significantly different from each other and completely different to those of droloxifene and the phenanthrene degradants. Compound **6** showed a major absorption band at 230 nm and a shoulder at 280 nm whereas **7** showed distinct maxima at 223, 282 and 328 nm [Fig. 6(a)].

LC-MS analysis showed a low-intensity mass spectrum for both compounds, but suggested an  $[M + H]^+$  ion at  $m/z$  317, corresponding to a relative molecular mass of 316 for each compound, indicating that the compounds were isomers. Loss of the *N,N*-dimethylaminoethyl group from droloxifene, to form the corresponding diphenolic compound, produces a species with the required relative molecular mass of 316. However, comparison with the authentic compound showed significantly different HPLC retention times and mass spectral fragmentations. NMR analysis was utilized for final confirmation of the two compound structures.

The proposed structures for **6** and **7** are shown in Fig. 7. A count of the carbons observed in the  $^{13}\text{C}$  NMR spectrum of **7**, the number of attached protons seen in the DEPT experiment, the exchangeable protons observed in the proton spectrum and a count of the oxygen atoms indirectly observed (a carbonyl and either a phenolic or vinyloxy group) gave a molecular formula of  $\text{C}_{22}\text{H}_{20}\text{O}_2$  and a relative molecular mass of 316, which agreed with the mass spectral data. The gradient COSY spectrum showed four spin systems [Figure 8(a)], three in the aromatic region. One spin system consisting of a pair of doublets in the aromatic region of the proton spectrum had a coupling constant of 16 Hz, which is indicative of *trans* vinyl protons. The long-range gradient HMQC [Fig. 8(b)] and NOE [Fig. 8(c)] data allowed placement of the non-protonated carbons and substituents on the naphthalene ring system. Finally, the exchangeable proton was attached to the phenolic carbon, resulting in the structure proposed for **7**. A lower concentration of **6** submitted for NMR analysis prevented as extensive an identity characterization as with **7**. However, a comparison of the COSY data showed the same four correlation patterns and similar carbon shifts. The main difference observed was a change in the coupling constant of the vinyl protons from 16 to 12 Hz, indicative of a change from *E* to *Z* configuration of the vinyl group. Hence the two compounds are an *E* and *Z* isomer pair (Fig. 7), which is supported by the mass spectral data.

The observed differences between the UV spectra of **6** and **7** deserve some comment. These two isomers differ, as determined by NMR spectroscopy, only in the configuration of their respective enone moieties, but they differ significantly in their UV spectral properties. A computational approach was used to try to model their UV spectra and, in doing so, lend support to the assignment of the proposed structures. A conformational search performed using the Sybyl ForceField computation yielded a family of eight *Z*-isomers for **6** and a family of eight *E*-isomers for **7**. Further optimization of these structures in gas phase using the Sybyl ForceField showed that the *E*-isomers could generally reach a much higher degree of coplanarity between the enone system and the naphthalene ring, whereas the *Z*-isomers had a much more orthogonal positioning of the enone system with respect to the naphthalene ring. It is worth mentioning that the structures obtained for the *E*-isomer are consistent with the observed NOE between the aromatic proton and the vinylic proton. The  $\omega_1$  torsional angle (Fig. 7) is always nearly coplanar for the *E*-isomer family of structures (close to  $30^\circ$ ), whereas it deviates significantly from coplanarity for the *Z*-isomer family of structures ( $50$ – $110^\circ$ ). Overall these results show that the observed differences in the UV spectra of these two isomeric compounds may be rationalized through this computational approach.

Referring to Fig. 6, the spectral simulations performed on each isomer indicated that, for the *Z* family of isomers

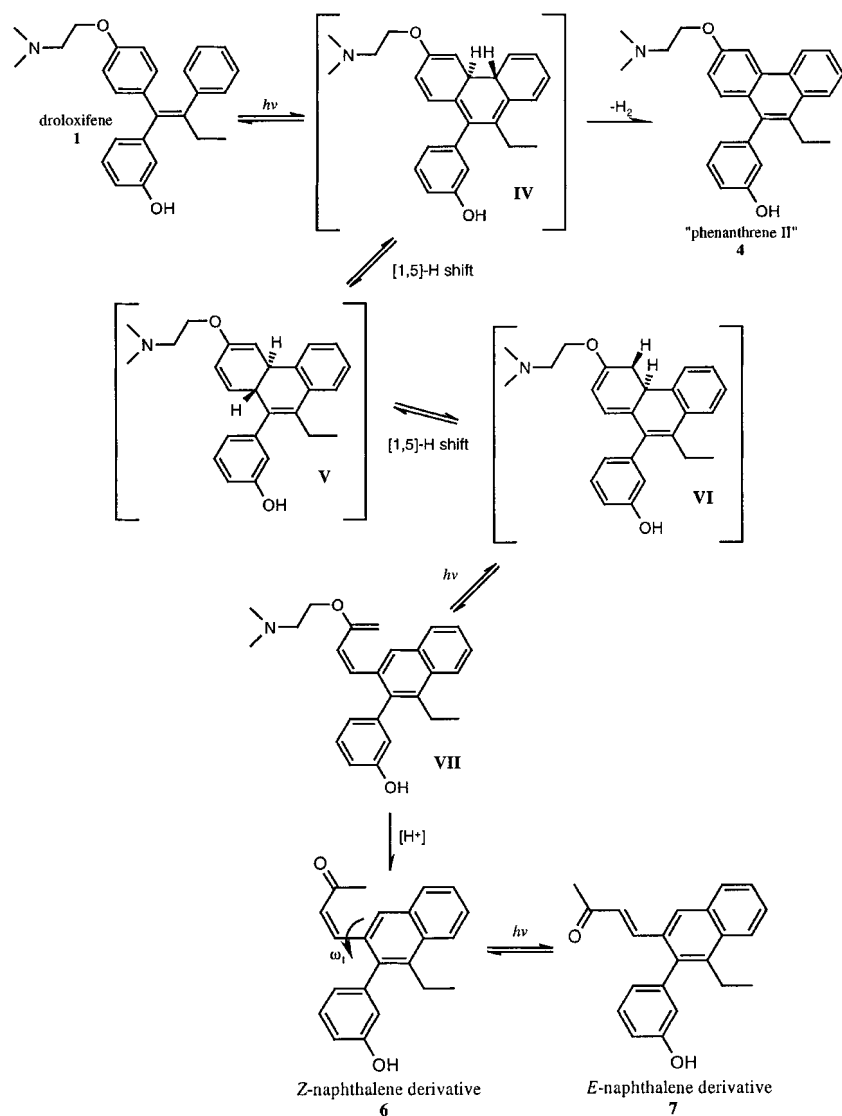


**Figure 7.** Proposed mechanism for the formation of naphthalene derivatives

(6), the 275–325 nm region either showed the presence of a poorly defined shoulder, as in the experimental spectrum, or the observed maximum in that region was relatively broad. Furthermore, a fairly high intensity ratio

between the maximum in the 220–240 nm region and that in the 275–325 nm region was invariably observed. It is realized, of course, that no single gas-phase simulated spectrum can be expected to reproduce an observed

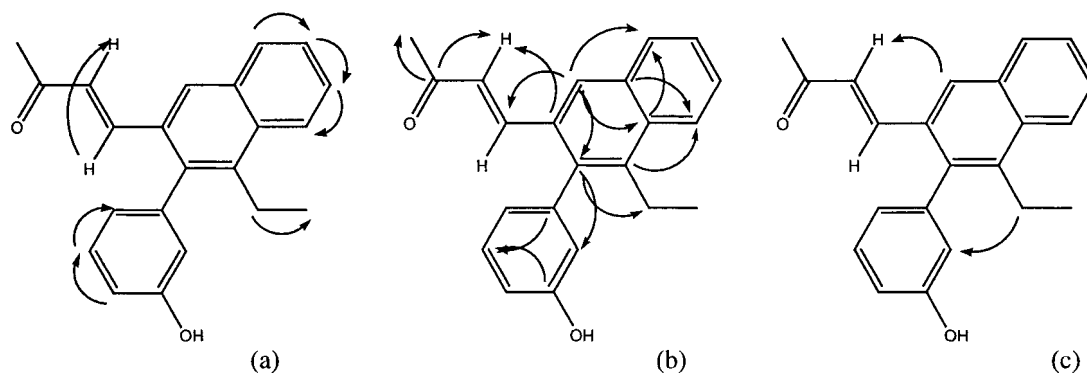


**Figure 8.** NMR correlations observed in the *E*-naphthalene isomer: (a) COSY connectivities; (b) long-range C to H connectivities; (c) NOE correlations

solution spectrum accurately, which would be the result of the absorption of several conformers. However, the agreement is fairly good between the computed and observed spectra, in the regions described.

Conversely, the *E* family of isomers (**7**) showed a consistently lower intensity ratio between the absorption maximum in the 220–240 nm region, and a well defined maximum observed in the 275–325 nm region as in the experimental spectra. Overall, both simulated spectra provide good backing for the structural assignments for these compounds.

A possible pathway for the formation of **6** and **7** must explain the experimental observations that (i) **6** and **7** are not formed at neutral or alkaline pH, even upon irradiation of the solution, and (ii) **6** and **7** are not formed at acidic pH in the absence of light.

The proposed mechanism for the formation of **6** and **7**, the *Z*- and *E*-naphthalene isomers respectively, is shown in Fig. 7. The ring closure, to generate phenanthrene II (**4**), is a well known occurrence for stilbene systems upon irradiation. The initial dihydrophenanthrene is the result of a conrotatory electrocyclic ring closure which converts a 1,3,5-hexatriene into a cyclohexadiene. This intermediate has been isolated for diethylstilbestrol.<sup>15</sup> This step, followed by removal of hydrogen atoms by dissolved molecular oxygen (or other hydrogen acceptors which might be present in the system), yields the phenanthrene derivative. This transformation is generally fairly rapid and, as mentioned, has served as the basis for post-column derivatization in the quantitation of tamoxifen and its derivatives in biological matrices.<sup>1</sup>

Referring to Fig. 7, dihydrophenanthrene IV could undergo sequential [1,5]-sigmatropic shifts to yield dihydrophenanthrene VI. Such a process would be thermally allowed as a suprafacial shift.<sup>16</sup> These steps are probably not too high in energy for cyclic systems, and they have indeed been reported at room temperature for cyclopentadienyl systems.<sup>17,18</sup> The last step of the sequence, leading to vinyl ether VII, is an electrocyclic ring opening from a 1,3-cyclohexadiene to a 1,3,5-hexatriene. Similar rearrangements have been reported to occur in steroid systems upon irradiation.<sup>19</sup>

The presence of an acidic environment is crucial to the sequence of events described, as the trapping of the vinyl ether must play a fundamental role in the formation of **6** and **7**. This process slows down as pH increases from 1.5 to 5, and it is not observed at pH 7. Indeed, the formation of **6** (*Z*-isomer) would result from an acid-catalyzed hydrolysis of VII, with concomitant loss of the alkyl chain. Finally, **7** would be formed by rapid isomerization of **6** induced by light. This is consistent with the experimental observation. Thus the acidic environment is ultimately driving the reaction sequence leading to **6** and **7** from the initial dihydrophenanthrene.

All the steps described above, after the initial ring closure leading to IV, appear likely to occur under the experimental conditions employed. In the absence of an

efficient hydrolysis step for VII, however, the latter intermediate may revert back to dihydrophenanthrene VI, which presumably would then revert to IV. This initial dihydrophenanthrene would then exclusively undergo a facile dehydrogenation to the corresponding phenanthrene derivative and the naphthalene derivatives would not be observed. It also would intuitively appear that this phenanthrene could be formed from any of the dihydrophenanthrene intermediates under the experimental conditions.

## CONCLUSION

An investigation into the photodecomposition of droloxifene was conducted. The results showed decay to be rapid, with the formation of its *Z*-isomer, several phenanthrene products and, in acidic media, two naphthalene derivatives. LC–MS was useful for the initial identification of the phenanthrene derivatives. Computational methods and comparison of chemical properties to structurally similar tamoxifen and related phenanthrenes were used ultimately to assign the structure of each phenanthrene product. Detailed NMR analysis was necessary to assign and confirm structures of the two naphthalene derivatives, which were unexpected photodecay products of droloxifene. Their structural assignments also correlate with properties predicted by computational methods. In addition to describing the photodecay mechanism and products of droloxifene, the present work also demonstrated the utility of computational methods in providing support for the structural elucidation of unknown decay products.

## Acknowledgements

The authors thank Dr Sally Gut for assistance with the interpretation of droloxifene decay mechanisms, Dr Frank DiCapua for assistance with some of the calculations and Dr Eugene Fiese for very helpful discussions throughout this work.

## REFERENCES

1. Nieder M, Jaeger H, *J. Chromatogr.* 1987; **413**: 207–217.
2. Jank P, Kern D, Huber HJ, Stanislaus F. In *Proceedings of 3rd European Congress on Biopharmacology and Pharmacokinetics*, vol. 1. 1987; 511–520.
3. Wilson S, Ruenitz PC, *J. Pharm. Sci.* 1993; **82**: 571–574.
4. Salamoun J, Macka M, Nechvatal M, Matousek M, Knesel L, *J. Chromatogr.* 1990; **514**: 179–187.
5. Ernst R, Bodenhausen G, Wokaun A, *Principles of Nuclear Magnetic Resonance in One and Two Dimensions*, pp. 400–489. Clarendon Press: Oxford, 1987.
6. SPARTAN Molecular Modeling Software, Version 5.1. Wavefunction, Irvine, CA. URL <http://www.wavefun.com/>
7. Sybyl Molecular Modeling Software, Version 6.3. Tripos, St. Louis, MO. URL <http://www.tripos.com/>

8. *CaChe Molecular Modeling Software, Release 4.0*. Oxford Molecular, Beaverton, OR. URL <http://www.oxmol.com/>
9. Poon GK, Bisset GMF, Mistry P, *J. Am. Soc. Mass Spectrom.* 1993; **4**: 588–595.
10. Mallory FB, Mallory CW, *Org. React. (N.Y.)* 1984; **30**: 1–456.
11. Mallory FB, Mallory CW, *J. Am. Chem. Soc.* 1972; **94**: 6041–6048.
12. Bao Z, Yang SK, *J. Chromatogr.* 1991; **536**: 245–249.
13. *CLogP, Medchem Project, Version 3.55 Using the 1996 Parameter set*. Pomona, CA. URL <http://www.biobyte.com/>
14. *LogKowwin, Version 1.57*. SRC, Syracuse, NY. URL [http://esc\\_plaza.syrres.com/](http://esc_plaza.syrres.com/)
15. Doyle TD, Benson WR, Filipescu N, *J. Am. Chem. Soc.* 1976; **98**: 3262–3267.
16. Woodward RB, Hoffman R, *The Conservation of Orbital Symmetry*. Verlag Chemie; Weinheim/Bergstrasse, 1970; 114–140.
17. McLean S, Haynes P, *Tetrahedron*, 1965; **21**: 2329–2342.
18. Childs RF, *Tetrahedron* 1982; **38**: 567–608.
19. Dauben WG, Fonken GJ, *J. Am. Chem. Soc.* 1959; **81**: 4060–4068.